Distributional properties of the typical cell of stationary iterated tessellations

Roland Maier Johannes Mayer Volker Schmidt

Universität Ulm
Abteilung Stochastik
D-89069 Ulm

October 6, 2003

Abstract

Distributional properties are considered of the typical cell of stationary iterated tessellations (SIT), which are generated by stationary Poisson-Voronoi tessellations (SPVT) and stationary Poisson line tessellations (SPLT), respectively. Using Neveu's exchange formula, the typical cell of SIT can be represented by those cells of its component tessellation hitting the typical cell of its initial tessellation. This provides a simulation algorithm without consideration of limits in space. It has been applied in order to estimate the probability densities of geometric characteristics of the typical cell of SIT generated by SPVT and SPLT. In particular, the probability densities of the number of vertices, the perimeter, and the area of the typical cell of such SIT have been determined.

Keywords Stochastic geometry; stationary tessellation; Palm calculus; Typical cell; iterated tessellation; Poisson Voronoi tessellation; Poisson line tessellation; simulation

Mathematics Subject Classification 2000: Primary 60D05; 68U20; Secondary 60G55

1 Introduction

The model assumptions of random tessellations like SPVT and SPLT are rather restrictive and in many cases they are not reflected by real data. For example, the spatial modelling of telecommunication access networks requires models, which take the spatial irregularity of the network architecture into account, see Gloaguen et al. [6] and the references therein. Thus, the need arises to construct more general models of random tessellations, which are still tractable from the computational point of view.

A fundamental operation on random tessellations producing new tessellations from old ones is the operation of iteration. Each cell of an initial tessellation is further subdivided into smaller cells by so-called component tessellations.

For SIT parametric representations of simple mean-value formulae concerning geometric characteristics of the typical cell can be derived. However, for many applications distributional properties of cell characteristics are required, which cannot, in general, be determined by closed formulae, and therefore have to be simulated.

In the present paper, distributional properties of the typical cell of SIT are considered. From the computational point of view, the most important classes of SIT are those constructed from SPVT and SPLT. Using Neveu's exchange formula, the typical cell of SIT can be represented by those cells of its component tessellation hitting the typical cell of its initial tessellation. This provides a simulation algorithm without consideration of limits in space. It has been applied in order to estimate the probability densities of geometric characteristics of the typical cell of SIT generated by SPVT and SPLT. In particular, the probability densities of the number of vertices, the perimeter, and the area of the typical cell of such SIT have been determined. From analytical formulae it is well known how the expectations of these geometric characteristics depend on the relationship between the expected total length of edges per unit area of the initial and component tessellations. The simulation results show a similar qualitative behaviour of the probability densities of these characteristics. The simulated probability densities can be used in order to develop statistical model tests for deciding the question, whether an SIT generated by SPVT and SPLT is suitable or not for oberserved empirical data.

The paper is organized as follows. In Section 2, the notion of a stationary random tessellation and the associated concept of its typical cell are recalled by using Palm calculus. In Section 3 a mathematical definition of SIT is given. Using Neveu's exchange formula, a representation of the typical cell of SIT provides the mathematical basis in order to estimate probability densities of geometric characteristics of the typical cell of SIT generated by SPVT and SPLT, respectively, from simulated data. Finally, in Section 4, some numerical examples are presented and discussed.

2 Some Preliminaries

In this section we recall some basic notion and notation of the theory of stationary random tessellations and its associated concept of the typical cell. More details can be found in Ambartzumian [1], Baccelli and Brémaud [2], Daley and Vere-Jones [4], Kallenberg [7], Matheron [11], Mecke [12], Miles [16], Møller [20], Schneider and Weil [24], and Stoyan et. al. [26] and the references therein.

2.1 Stationary random tessellations

One possible way to introduce stationary random tessellations in the plane $\mathbb{R}^2$ is to define them as point processes in the space of all nonempty closed subsets of $\mathbb{R}^2$.

Roughly speaking, a random tessellation is a random subdivision of $\mathbb{R}^2$ into non-overlapping polygons called the *cells* of the tessellation.

More formally, let $(\Omega, \mathcal{A}, \mathbb{P})$ be an arbitrary probability space. Furthermore, let $\mathcal{F}$ be the space of all nonempty closed sets in $\mathbb{R}^2$. An important subclass of $\mathcal{F}$ is the family $\mathcal{P}$ of all polygons, i.e., the family of all compact sets with nonempty interior, which are finite intersections of closed half-planes.

For any random set $\Xi : \Omega \to \mathcal{F}$, let δ_Ξ denote the Dirac measure of Ξ. Then, a *random tessellation* may be defined as a simple point process $X = \sum_n \delta_{\Xi_n}$ in $\mathcal{F}$ fulfilling the following conditions with probability 1:

(i) $\operatorname{int} \Xi_n \neq \emptyset$ for all n, where $\operatorname{int} \Xi_n$ denotes the interior of the set Ξ_n,

(ii) Ξ_n are compact and convex for all n,

(iii) $\operatorname{int} \Xi_{n_1} \cap \operatorname{int} \Xi_{n_2} = \emptyset$ if $n_1 \neq n_2$, and

(iv) $\bigcup_{n=1}^\infty \Xi_n = \mathbb{R}^2$.

Let $\{\theta_x, x \in \mathbb{R}^2\}$ be a flow on Ω, i.e. a random field with values in Ω such that $\theta_x \circ \theta_y = \theta_{x+y}$ for $x, y \in \mathbb{R}^2$ and θ_0 is the identity on Ω. Then a random tessellation X in $\mathbb{R}^2$ is called *stationary* if

$$X(\theta_x \omega, B) = X(\omega, B + x) \quad \text{and} \quad \mathbb{P} \circ \theta_x = \mathbb{P}$$

for each $x \in \mathbb{R}^2$, $\omega \in \Omega$ and each Borel set $B \subset \mathcal{F}$.

We conclude this section with two important examples of stationary random tessellations, which have been intensively studied in the literature; see, for example, Miles [15, 16, 17, 18], Møller [20], Okabe et. al. [21] and Stoyan et. al. [26] and the references therein.

Let $X' = \sum_n \delta_{\xi_n}$ be a stationary Poisson point process (SPPP) in $\mathbb{R}^2$ of intensity γ. Then a random tessellation $X = \sum_n \delta_{\Xi_n}$ with

$$\Xi_n = \{x \in \mathbb{R}^2 : \|x - \xi_n\| \leq \|x - \xi_m\| \ \forall m \neq n\}, \tag{2.1}$$

where $\|x - y\|$ denotes the Euclidean distance of $x, y \in \mathbb{R}^2$, is called a stationary Poisson-Voronoi tessellation (SPVT) in $\mathbb{R}^2$ with parameter γ. The point ξ_n is called the *nucleus* of the *Voronoi cell* Ξ_n; see Figure 1.

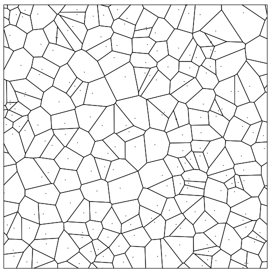

(a) SPVT

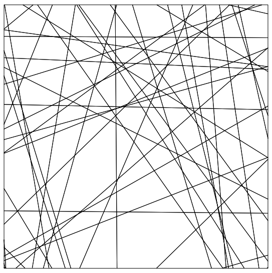

(b) SPLT

Figure 1: Random Tessellations

Regarding the simulation of the typical cell of a SPVT (see Section 3 below), it is convenient to switch to polar coordinates, i.e., to represent X' as an independently marked point process $X' = \sum_n \delta_{(R_n,\Phi_n)}$ in $\mathbb{R}_+ \times [0, 2\pi)$, where

$$R_n = \sqrt{-\sum_{i=1}^{n} \log U_i / \pi\,\gamma}\,, \tag{2.2}$$

$\{U_n\}$ and $\{\Phi_n\}$ are independent sequences of independent random variables $U_n \sim \mathrm{U}[0,1]$ and $\Phi_n \sim \mathrm{U}[0,2\pi)$, respectively; see Quine and Watson [22].

A random tessellation, which is induced by a stationary Poisson line process (SPLP) X' in $\mathbb{R}^2$ of intensity γ and non-degenerate orientation distribution G, is called a stationary Poisson line tessellation (SPLT) with parameter γ and orientation distribution G. Notice that X' can be represented as a stationary, independently marked PPP $X' = \sum_n \delta_{(R_n,\Phi_n)}$ in $\mathbb{R} \times [0, \pi)$, i.e. each line is identified with its signed perpendicular distance R_n from the origin and its orientation Φ_n; see Figure 1.

2.2 Palm calculus and typical cell

The mathematical concept of the typical cell of stationary random tessellation may be introduced with the aid of Palm calculus. Intuitively, the typical cell is a random polygon with the distribution of a randomly chosen cell, where all cells have equal chance of being selected. To give an exact mathematical definition of the typical cell, for each cell Ξ_n choose an *associated point* $c(\Xi_n)$, i.e. a measurable mapping $c : \mathcal{P} \to \mathbb{R}^2$ satisfying $c(P + x) = c(P) + x$ for all $x \in \mathbb{R}^2$ and $P \in \mathcal{P}$. In the case of a SPLT, for example, the associated points of the cells can be their smallest vertices in the sense of the lexicographical order. However, in the case of a SPVT, it is convenient to choose the nucleii of the Voronoi cells as associated points.

Then, a random tessellation $X = \sum_n \delta_{\Xi_n}$ can be represented as a marked point process

$$X = \sum_n \delta_{(c(\Xi_n),\Xi_n - c(\Xi_n))}$$

in $\mathbb{R}^2$ with marks in the space $\mathcal{P}_o = \{P \in \mathcal{P} : c(P) = o\}$ of all polygons "centered" at the origin $o \in \mathbb{R}^2$.

In the following, we require that X is stationary. Let $|\cdot|$ denote the Lebesgue measure in $\mathbb{R}^2$. The constant λ_X defined by

$$\lambda_X\,|B| = \mathbb{E}\sum\nolimits_n \mathbb{1}\big(c(\Xi_n) \in B\big)$$

for each Borel set $B \subset \mathbb{R}^2$ is called the *intensity* of X and is assumed to be positive and finite. Consider the *Campbell measure* $\mathcal{C}_X$ in $\mathbb{R}^2 \times \mathcal{P}_o \times \Omega$ defined by

$$\mathcal{C}_X(B \times L \times A) = \int_\Omega \int_{B\times L} \mathbb{1}\,(\omega \in A)\, X(\omega, \mathrm{d}(x,P))\, \mathbb{P}(\mathrm{d}\omega)\,. \tag{2.3}$$

Then, there exists a uniquely determined probability measure $\mathbb{P}_X$ in $\mathcal{P}_o \times \Omega$ called *Palm probability* of X such that

$$\mathcal{C}_X(B \times L \times A) = \lambda_X \int_B \mathbb{P}_X(L \times \theta_{-x}A)\,\mathrm{d}x\,, \tag{2.4}$$

where $\theta_{-x}A = \{\theta_{-x}\omega : \omega \in A\}$. Furthermore, define the *Palm mark distribution* $\mathbb{Q}_X$ as the projection of $\mathbb{P}_X$ onto the first component of the product space $\mathcal{P}_o \times \Omega$, i.e.

$$\mathbb{Q}_X(L) = \mathbb{P}_X(L \times \Omega)\,. \tag{2.5}$$

A random polygon $\Xi_X \sim \mathbb{Q}_X$ is called the *typical cell* of X. If Ω is identified with the space $\mathrm{N}(\mathbb{R}^2 \times \mathcal{P}_o)$ of all locally finite counting measures in $\mathbb{R}^2 \times \mathcal{P}_o$, then the *Palm distribution* $\mathbb{P}_X^{o,P}$ of X can be introduced by disintegration of $\mathbb{P}_X$, i.e., there exists a $\mathbb{Q}_X$-a.s. uniquely determined regular family $\{\mathbb{P}_X^{o,P}\}$ of probability measures in $\mathrm{N}(\mathbb{R}^2 \times \mathcal{P}_o)$ s.t.

$$\mathbb{P}_X(L \times A) = \int_L \mathbb{P}_X^{o,P}(A)\,\mathbb{Q}_X(\mathrm{d}P)\,. \tag{2.6}$$

Analogously to (2.3)-(2.6), n-th order Palm measures can be derived from corresponding higher order Campbell measures defined in $(\mathbb{R}^2 \times \mathcal{P}_o)^n \times \Omega$; see Kallenberg [7]. The mathematical concept of the typical cell in (2.5) admits the following interpretation. If X is ergodic, then (2.4) implies that for any measurable $f : \mathcal{P}_o \times \Omega \to \mathbb{R}_+$, we have with probability 1

$$\begin{aligned}\int_{\mathcal{P}_o\times\Omega} & f(P,\omega)\,\mathbb{P}_X(\mathrm{d}(P,\omega)) \\ &= \lim_{k\to\infty} \frac{1}{X(\omega, B_k \times \mathcal{P}_o)} \int_{B_k\times\mathcal{P}_o} f(P, \theta_x\omega)\, X(\omega, \mathrm{d}(x,P))\,,\end{aligned} \tag{2.7}$$

where $B_k = b(o, r_k)$ is the closed ball with centre at the origin and radius $r_k > 0$ such that $\lim_{k\to\infty} r_k = \infty$. Thus, the Palm probability $\mathbb{P}_X(\mathcal{P}_o \times \cdot)$ can be interpreted as the probability measure in Ω from the perspective of the *typical associated point* of X. In view of different simulation techniques, (2.7) implies that the spatial average of any cell characteristic of a tessellation X coincide with the corresponding expected value under the Palm probability $\mathbb{P}_X$ provided that X is ergodic. Thus, algorithms for sampling the typical cell, which are based on a sequence of independent realizations of the Palm version of X can be applied.

An immediate consequence of (2.4) is the *Campbell-Mecke formula*, which states that for any measurable $f : \mathbb{R}^2 \times \mathcal{P}_o \times \Omega \to \mathbb{R}_+$

$$\int_{\mathcal{P}_o\times\Omega}\int_{\mathbb{R}^2} f(x,P,\omega)\,\mathrm{d}x\,\mathbb{P}_X(\mathrm{d}(P,\omega)) \\ = \frac{1}{\lambda_X}\int_{\Omega}\int_{\mathbb{R}^2\times\mathcal{P}_o} f(x,P,\theta_x\omega)\,X(\omega,d(x,P))\,\mathbb{P}(\mathrm{d}\omega)\,. \tag{2.8}$$

Furthermore, using (2.8) one can prove *Neveu's exchange formula.* Indeed, let X_1 and X_2 be arbitrary stationary random tessellations in $\mathbb{R}^2$ with intensities λ_{X_1} and λ_{X_2}, respectively. Then, for any measurable $f : \mathbb{R}^2 \times \mathcal{P}_o^2 \times \Omega \to \mathbb{R}_+$,

$$\begin{aligned} &\lambda_{X_1}\int_{\mathcal{P}_o\times\Omega}\int_{\mathbb{R}^2\times\mathcal{P}_o} f(-x,P,P',\theta_x\omega)\,X_2(\omega,\mathrm{d}(x,P'))\,\mathbb{P}_{X_1}(\mathrm{d}(P,\omega)) \\ &= \lambda_{X_2}\int_{\mathcal{P}_o\times\Omega}\int_{\mathbb{R}^2\times\mathcal{P}_o} f(x,P,P',\omega)\,X_1(\omega,\mathrm{d}(x,P))\,\mathbb{P}_{X_2}(\mathrm{d}(P',\omega))\,; \end{aligned} \tag{2.9}$$

see, for example, Baccelli and Brémaud [2], Schmidt and Serfozo [25].

3 Stationary iterated tessellations

In this section we consider the iteration of random tessellations, where each cell of an initial tessellation is further subdivided into smaller cells by so-called component tessellations; see, for example, Ambartzumian [1], Baccelli et. al. [2], Kendall and Mecke [8], Maier and Schmidt [9], Mecke [13], Miles and Mackisack [19], Santaló [23], and Weiss and Nagel [27].

3.1 Definition

Let $X_0 = \sum_n \delta_{\Xi_n}$ be a stationary random tessellation and let $\{X_n\}$, $n \geq 1$, be a sequence of stationary random tessellations $X_n = \sum_\nu \delta_{\Xi_{n,\nu}}$, which are *exchangeable*, i.e.

$$(X_1,\ldots,X_n) \overset{\mathrm{d}}{=} (X_{\pi(1)},\ldots,X_{\pi(n)}) \tag{3.1}$$

for each n and each permutation $\pi : \{1, \ldots, n\} \to \{1, \ldots, n\}$. Moreover, let X_0 and $\{X_n\}$ be independent. Then, the point process X in $\mathcal{F}$ defined by

$$X(B) = \sum\nolimits_{n,\nu} \delta_{\Xi_{n,\nu} \cap \Xi_n}(B) \, \mathbb{1}(\text{int } \Xi_{n,\nu} \cap \text{int } \Xi_n \neq \emptyset) \tag{3.2}$$

for each Borel set $B \subset \mathcal{F}$ is called an SIT with stationary *initial tessellation* X_0 and stationary *component tessellations* $\{X_n\}$. In particular, an SIT X is said to be a X_0/X_1-*superposition* if the sequence $\{X_n\}$ of component tessellations satisfies $X_1 = X_2 = \ldots$; see Figure 2.

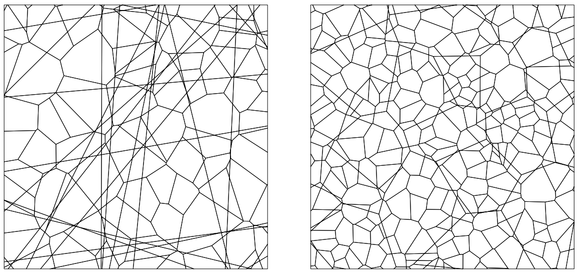

(a) SPLT/SPVT (b) SPVT/SPVT

Figure 2: X_0/X_1-superposition

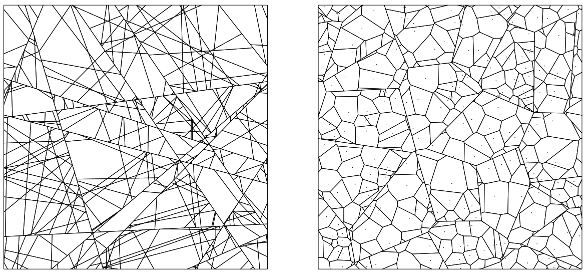

(a) SPLT/SPLT (b) SPVT/SPVT

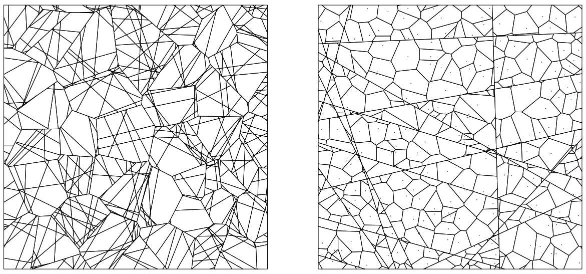

(c) SPVT/SPLT (d) SPLT/SPVT

Figure 3: X_0/X_1-nesting

An SIT is called X_0/X_1-*nesting* if the sequence $\{X_n\}$ of component tessellations consists of iid ST; see Figure 3. Notice that in both cases condition (3.1) is fulfilled.

3.2 Representation of the typical cell

The exchange formula (2.9) can be used in order to represent the typical cell of an arbitrary SIT by those cells of the component tessellation hitting the typical cell of the initial tessellation. Notice that this representation only depends on the one-dimensional marginal distribution of the sequence $\{X_n\}$. In particular, we get the same formula for superposition and for nesting.

Proposition 3.1 Let X be an SIT with initial tessellation X_0 and component tessellations $\{X_n\}$, where the intensities of X_0 and X are denoted by λ_{X_0} and λ_X, respectively. Then, for any measurable $h : \mathcal{P}_o \to \mathbb{R}_+$,

$$\begin{aligned}&\int_{\mathcal{P}_o} h(P)\,\mathbb{Q}_X(\mathrm{d}P)\\ &\quad= \frac{\lambda_{X_0}}{\lambda_X}\int_{\mathcal{P}_o}\mathbb{E}\Big[\sum\nolimits_n h(\Xi_{1,n}\cap P)\,\mathbb{1}(\mathrm{int}\,\Xi_{1,n}\cap\mathrm{int}\,P\neq\emptyset)\Big]\,\mathbb{Q}_{X_0}(\mathrm{d}P)\,,\end{aligned}$$

where $\Xi_{1,1}, \Xi_{1,2}, \ldots$ are the cells of the component tessellation X_1.

Proof Suppose that the tessellations X_1 and X_2 in (2.9) are equal to X_0 and X, respectively. Then, inserting the function $f : \mathbb{R}^2 \times \mathcal{P}_o^2 \times \Omega \to \mathbb{R}_+$ with

$$f(x, P, P', \omega) = h(P')\,\mathbb{1}(\mathrm{int}\,P' \cap \mathrm{int}\,(P + x) \neq \emptyset)$$

into (2.9), the statement follows having in mind that the tessellations X_0 and X_1 are independent.

3.3 A consistent estimator

Proposition 3.1 leads to the following procedure, which can be used to estimate characteristics of the typical cell of the SIT X. Let $\{\Xi_{X_0}^{(i)}\}$ be a sequence of iid random polygons $\Xi_{X_0}^{(i)} \sim \mathbb{Q}_{X_0}$, and let $\{X_1^{(i)}\}$ be a sequence of iid tessellations $X_1^{(i)} = \sum_n \delta_{\Xi_{1,n}^{(i)}}$ with $X_1^{(i)} \overset{\mathrm{d}}{=} X_1$, independent of $\{\Xi_{X_0}^{(i)}\}$. Then, the ratio

$$\widehat{H}_X^{(j)} = \frac{\sum_{i=1}^{j}\sum_{n=1}^{\infty} h(\Xi_{1,n}^{(i)}\cap\Xi_{X_0}^{(i)})\,\mathbb{1}(\mathrm{int}\,\Xi_{1,n}^{(i)}\cap\mathrm{int}\,\Xi_{X_0}^{(i)}\neq\emptyset)}{\sum_{i=1}^{j}\sum_{n=1}^{\infty}\mathbb{1}(\mathrm{int}\,\Xi_{1,n}^{(i)}\cap\mathrm{int}\,\Xi_{X_0}^{(i)}\neq\emptyset)} \tag{3.3}$$

is a consistent estimator for the expectation $\int_{\mathcal{P}_o} h(P)\,\mathbb{Q}_X(\mathrm{d}P)$ as $j\to\infty$. Indeed, from the law of large numbers we have with probability 1

$$\frac{1}{j}\sum_{i=1}^{j}\sum_{n=1}^{\infty} h(\Xi_{1,n}^{(i)}\cap\Xi_{X_0}^{(i)})\,\mathbb{1}\,(\mathrm{int}\,\Xi_{1,n}^{(i)}\cap\mathrm{int}\,\Xi_{X_0}^{(i)}\neq\emptyset)\longrightarrow$$

$$\int_{\mathcal{P}_o}\mathbb{E}\left[\sum_{n=1}^{\infty} h(\Xi_{1,n}\cap P)\,\mathbb{1}\,(\mathrm{int}\,\Xi_{1,n}\cap\mathrm{int}\,P\neq\emptyset)\right]\mathbb{Q}_{X_0}(\mathrm{d}P)$$

and

$$\frac{1}{j}\sum_{i=1}^{j}\sum_{n=1}^{\infty}\mathbb{1}\,(\mathrm{int}\,\Xi_{1,n}^{(i)}\cap\mathrm{int}\,\Xi_{X_0}^{(i)}\neq\emptyset)\longrightarrow\frac{\lambda_X}{\lambda_{X_0}}\,.$$

Thus, by Proposition 3.1, we have $\lim_{j\to\infty}\widehat{H}_X^{(j)}=\int_{\mathcal{P}_o} h(P)\,\mathbb{Q}_X(\mathrm{d}P)$ with probability 1. However, the estimator $\widehat{H}_X^{(j)}$ defined by (3.3) is only applicable if the Palm mark distribution $\mathbb{Q}_{X_0}$ of the initial tessellation X_0 can be simulated. This requirement is guaranteed if X_0 is a stationary PVT and PLT. In these important cases the Palm distributions of the generating Poisson processes are explicitly known as described below.

In principle, the i.i.d. sequence $\{\Xi_{X_0}^{(i)}\}$ of typical cells $\Xi_{X_0}^{(i)}\sim\mathbb{Q}_{X_0}$ can be replaced by the sequence of cells of a single sample of X_0 provided that the stationary initial tessellation X_0 is ergodic. However, the disadvantage of this approach is that the variance of the estimator considered in (3.3) is much more complicated than in the case of direct i.i.d. sampling of the typical cell of the initial tessellation X_0.

3.4 Application of Slivnyak's theorem

Suppose that X_0 is a stationary PVT induced by the PPP X'. Then, *Slivnyak's theorem* states that the Palm distribution $\mathbb{P}_{X'}^o$ of the generating Poisson process X' is given by

$$\mathbb{P}_{X'}^o(A)=\mathbb{P}(X'+\delta_o\in A)\,;$$

see, for example, Schneider and Weil [24], Stoyan et. al. [26]. Algorithms for simulating the typical cell of X_0 under the Palm distribution $\mathbb{P}_{X'}^o$ of X', which are based on radial simulation can be applied; see the monograph of Okabe et. al. [21], where different simulation techniques are discussed and an overview of the literature is given.

In order to sample the typical cell of a stationary PLT X_0 induced by the PLP X' with orientation distribution G, it is convenient to map the generating process X' under the measurable transformation $T:\mathrm{N}(\mathbb{R}\times[0,\pi))\to\mathrm{N}(\mathbb{R}^2\times[0,\pi)^2)$ into the generating process X'' in $\mathbb{R}^2\times[0,\pi)^2$ given by

$$X''=TX'=\sum\nolimits_{n_1<n_2}\delta_{\mathcal{T}^{-1}(R_{n_1},R_{n_2},\Phi_{n_1},\Phi_{n_2})}\,,$$

where the transformation $\tau : \mathbb{R}^2 \times [0,\pi)^2 \to \mathbb{R}^2 \times [0,\pi)^2$ is given by

$$\begin{pmatrix} r_1 \\ r_2 \\ \psi_1 \\ \psi_2 \end{pmatrix} = \tau(x,y,\phi_1,\phi_2) = \begin{pmatrix} \cos\phi_1 & \sin\phi_1 & 0 & 0 \\ \cos\phi_2 & \sin\phi_2 & 0 & 0 \\ 0 & 0 & 1 & 0 \\ 0 & 0 & 0 & 1 \end{pmatrix} \begin{pmatrix} x \\ y \\ \phi_1 \\ \phi_2 \end{pmatrix} \tag{3.4}$$

with Jacobi determinant

$$\left| \frac{\partial\, \tau(x,y,\phi_1,\phi_2)}{\partial x\, \partial y\, \partial \phi_1\, \partial \phi_2} \right| = |\sin(\phi_1 - \phi_2)|\,.$$

Consider $\mathbb{P}_{X''}$ as a probability measure in $[0,\pi)^2 \times \mathrm{N}(\mathbb{R}^2 \times [0,\pi)^2)$. Then, applying Slivnyak's theorem to the 2-fold Palm distribution $\mathbb{P}_{X'}^{(0,\phi_1),(0,\phi_2)}$ in $\mathrm{N}(\mathbb{R} \times [0,\pi))$ of the Poisson process X' gives

$$\begin{aligned}
\mathbb{P}_{X''}(L_1 \times L_2 \times A) &\overset{(2.6)}{=} \int_{L_1 \times L_2} \mathbb{P}_{X''}^{\tau^{-1}(0,0,\phi_1,\phi_2)}(A)\, \mathbb{Q}_{X''}(\mathrm{d}\phi_1 \times \mathrm{d}\phi_2) \\
&\overset{(3.4)}{=} \int_{L_1 \times L_2} \mathbb{P}_{X'}^{(0,\phi_1),(0,\phi_2)}(T^{-1}A)\, \mathbb{Q}_{X''}(\mathrm{d}\phi_1 \times \mathrm{d}\phi_2) \\
&= \int_{L_1 \times L_2} \mathbb{P}(X' + \delta_{(0,\phi_1)} + \delta_{(0,\phi_2)} \in T^{-1}A)\, \mathbb{Q}_{X''}(\mathrm{d}\phi_1 \times \mathrm{d}\phi_2) \\
&= \int_{L_1 \times L_2} \mathbb{P}(X'' + \delta_{(o,(\phi_1,\phi_2))} \in A)\, \mathbb{Q}_{X''}(\mathrm{d}\phi_1 \times \mathrm{d}\phi_2)\,,
\end{aligned}$$

where the distribution $\mathbb{Q}_{X''}$ is given by

$$\mathbb{Q}_{X''}(L_1 \times L_2) = \frac{\displaystyle\int_{L_1}\int_{L_2} |\sin(\phi_1 - \phi_2)| G(\,\mathrm{d}\phi_1)\, G(\,\mathrm{d}\phi_1)}{\displaystyle\int_{[0,\pi)}\int_{[0,\pi)} |\sin(\phi_1 - \phi_2)| G(\,\mathrm{d}\phi_1)\, G(\,\mathrm{d}\phi_1)}\,; \tag{3.5}$$

see, for example, Mecke [13], Miles [15].

This yields a two-step mechanism for sampling the typical cell of X_0 provided the orientation distribution G can be simulated. First simulate a random vector $(\Psi_1, \Psi_2) \sim \mathbb{Q}_{X''}$ given by (3.5), independent of X'. Given a realization (ψ_1, ψ_2) of (Ψ_1, Ψ_2) generate a sample of $X'' + \delta_{(o,(\psi_1,\psi_2))}$ by simulating $X' + \delta_{(0,\psi_1)} + \delta_{(0,\psi_2)}$. Then, the cell centered at the origin is a realization of the typical cell of X_0, where the same simulation methods as in the case of PVT are applicable. Another simulation method of the typical cell is presented in George [5].

4 Numerical examples

Using the simulation techniques explained in the previous section, provided by the framework described in Mayer et al. [10], we simulated 10 000 000 samples from the typical cell of X_0/X_1-nesting generated by SPVT and SPLT with orientation distribution $G = \mathrm{U}[0,\pi)$. From these samples, distributional characteristics of the typical cell as the number of vertices, the perimeter and the area have been analyzed.

For $i = 0, 1$, let $\lambda_i^{(0)}$, $\lambda_i^{(1)}$ and $\lambda_i^{(2)}$ denote the expected number of vertices, edge midpoints and associated points of cells of X_i per unit area, respectively. Moreover, let N, U and A denote the number of vertices, the perimeter and the area of the typical cell of a X_0/X_1-nesting, respectively. Their expectations are denoted by $\overline{N}$, $\overline{U}$ and $\overline{A}$, respectively. Then

$$\overline{N} = 2 + 2\,\frac{\lambda_0^{(0)} + \lambda_1^{(0)} + \frac{2}{\pi}L_{A,0}L_{A,1}}{\lambda_0^{(2)} + \lambda_1^{(2)} + \frac{2}{\pi}L_{A,0}L_{A,1}}\,, \tag{4.6}$$

$$\overline{U} = 2\,\frac{L_{A,0} + L_{A,1}}{\lambda_0^{(2)} + \lambda_1^{(2)} + \frac{2}{\pi}L_{A,0}L_{A,1}}\,, \tag{4.7}$$

$$\overline{A} = \frac{1}{\lambda_0^{(2)} + \lambda_1^{(2)} + \frac{2}{\pi}L_{A,0}L_{A,1}}\,, \tag{4.8}$$

where $L_{A,i}$ denotes the expected total length of edges of X_i per unit area; see, for example Mecke [13], Santaló [23], Weiss and Nagel [27]. In the case of a SPLT with parameter γ, we have

$$\lambda^{(0)} = \frac{\gamma^2}{\pi}\,, \qquad \lambda^{(1)} = \frac{2\gamma^2}{\pi}\,, \qquad \lambda^{(2)} = \frac{\gamma^2}{\pi}\,, \qquad L_A = \gamma\,, \tag{4.9}$$

whereas, in the case of a SPVT with parameter γ,

$$\lambda^{(0)} = 2\gamma\,, \qquad \lambda^{(1)} = 3\gamma\,, \qquad \lambda^{(2)} = \gamma\,, \qquad L_A = 2\sqrt{\gamma}\,; \tag{4.10}$$

see, for example, the monograph of Stoyan et. al. [26] and the references therein. According to formulae (4.6) - (4.10), the expected number of vertices $\overline{N}$, the expected perimeter $\overline{U}$ and the expected area $\overline{A}$ of the typical cell of X_0/X_1-nestings generated by SPVT or SPLT are depicted in Figure 4 as a function of $x = L_{A,1}/L_{A,0}$, where we put $L_{A,0} = 1$. Obviously, if $x = 0$, the geometrical characteristics of the typical cell of X_0/X_1-nesting coincide with the corresponding cell characteristics of X_0 since no iteration takes place. As the value of x increases, the cell characteristics of X_0/X_1-nesting are more and more influenced by X_1. Since a SPLT/SPLT-superposition is again a SPLT, the expected number of vertices $\overline{N}$ of a SPLT/SPLT-nesting does not depend on x; see Figure 4(a). Another obvious fact, which is reflected by Figure 4, is that the values of $\overline{N}$, $\overline{U}$ and $\overline{A}$ of SPLT/SPVT-nesting and SPVT/SPLT-nesting coincide provided that $L_{A,0} = L_{A,1}$.

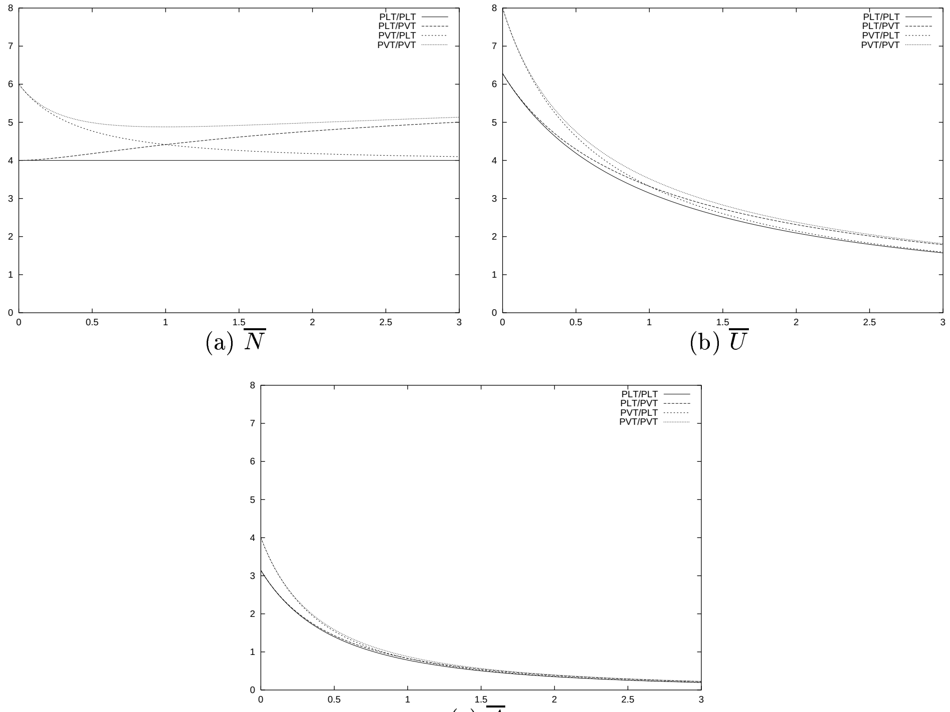

(a) $\overline{N}$ (b) $\overline{U}$

(c) $\overline{A}$

Figure 4: $\overline{N}$, $\overline{U}$, and $\overline{A}$ as a function of $x = L_{A,1}/L_{A,0}$ with $L_{A,0} = 1$.

The qualitative behaviour of the mean characteristics $\overline{N}$, $\overline{U}$ and $\overline{A}$ is also shown by their simulated values; see Table 1. The simulation results we obtained for $\overline{N}$, $\overline{U}$ and $\overline{A}$ are very close to the corresponding known theoretical values. For example, in the case of SPVT/SPLT-nesting with $L_{A,0} = 1$ and $L_{A,1} = 2$, we get from (4.6) - (4.10)

$$\overline{N} \approx 4.178796\,, \qquad \overline{U} \approx 2.145555\,, \qquad \overline{A} \approx 0.357593\,.$$

The estimates of distributional parameters of the typical cell given in Table 1 reflect the strong dependence of a X_0/X_1-nesting on the choice of X_0 and X_1 and the ratio $L_{A,1}/L_{A,0}$. For example, in the case $L_{A,0} = 1$ and $L_{A,1} = 2$, the minimum values of $\overline{N}$, $\overline{U}$ and $\overline{A}$ were achieved for SPLT/SPLT-nesting, whereas we received the corresponding maximum values for SPVT/SPVT-nesting. Furthermore, compared with the theoretical values of $\overline{N}$, $\overline{U}$ and $\overline{A}$ in the case of SPLT and SPVT with $L_A = 3$ given by

$$\overline{N} = 4\,, \qquad \overline{U} = 2\pi/3 \approx 2.09440\,, \qquad \overline{A} = \pi/9 \approx 0.34907$$

and

$$\overline{N} = 6\,, \qquad \overline{U} = 8/3 \approx 2.66667\,, \qquad \overline{A} = 4/9 \approx 0.44444\,,$$

	X_0/X_1-nesting	expectation	variance	minimum	maximum
N	SPLT/SPLT	4.000003 (3.999736)	0.934427 (0.934354)	3 (3)	12 (12)
	SPVT/SPLT	4.178746 (4.771928)	1.200106 (1.954103)	3 (3)	13 (14)
	SPLT/SPVT	4.772476 (4.179017)	1.953845 (1.200118)	3 (3)	14 (12)
	SPVT/SPVT	4.990519 (4.990592)	2.021023 (2.020552)	3 (3)	15 (16)
U	SPLT/SPLT	2.093663 (4.187006)	3.214070 (12.853061)	0.000000 (0.000000)	23.092143 (57.381293)
	SPVT/SPLT	2.144681 (4.630830)	2.768258 (7.262584)	0.000000 (0.000001)	14.326001 (18.104901)
	SPLT/SPVT	2.315988 (4.294556)	1.816681 (11.092893)	0.000001 (0.000002)	9.197925 (28.037479)
	SPVT/SPVT	2.377990 (4.755921)	1.584826 (6.332930)	0.000001 (0.000000)	8.070871 (16.268808)
A	SPLT/SPLT	0.348745 (1.394372)	0.477287 (7.643158)	0.000000 (0.000000)	35.992564 (193.768792)
	SPVT/SPLT	0.357426 (1.543865)	0.354526 (2.936430)	0.000000 (0.000000)	12.905172 (21.949146)
	SPLT/SPVT	0.386145 (1.432555)	0.183716 (5.680859)	0.000000 (0.000000)	5.830355 (55.527161)
	SPVT/SPVT	0.396446 (1.585253)	0.160255 (2.559065)	0.000000 (0.000000)	4.583114 (18.324242)

Table 1: Estimates of distributional parameters of the typical cell for X_0/X_1-nesting with $L_{A,0} = 1$ and $L_{A,1} = 2$ ($L_{A,1} = 1/2$)

respectively, all simulated values of $\overline{N}$, $\overline{U}$ and $\overline{A}$ of the considered X_0/X_1-nestings are roughly between these values.

The variability of the geometrical characteristics is expressed by the estimated variance and the difference between the maximum and minimum. The lowest and highest variability of N was received for SPLT/SPLT-nesting and SPVT/SPVT-nesting, respectively. However, the minimum and maximum variability of U and A was obtained for SPVT/SPVT-nesting and SPLT/SPLT-nesting, respectively. The estimates for the expectation and variance of N of SPLT/SPVT-nesting and SPVT/SPLT-nesting show also the strong dependence of a X_0/X_1-nesting on the choice of X_0 and X_1 and the ratio $L_{A,1}/L_{A,0}$, see the discussion below. The estimated expectation and variance of N of SPLT/SPVT-nesting with $L_{A,0} = 1$ and $L_{A,1} = 2$ are close to the corresponding values of N of SPVT/SPLT-nesting with $L_{A,0} = 1$ and $L_{A,1} = 1/2$.

Figure 5 shows estimates for characteristics of N for X_0/X_1-nestings with $L_{A,0} = 1$ and $L_{A,1} = 2$. In the case of SPLT/SPLT-nesting the dominating cell shapes are triangles and quadrangles, see Figure 5(a).

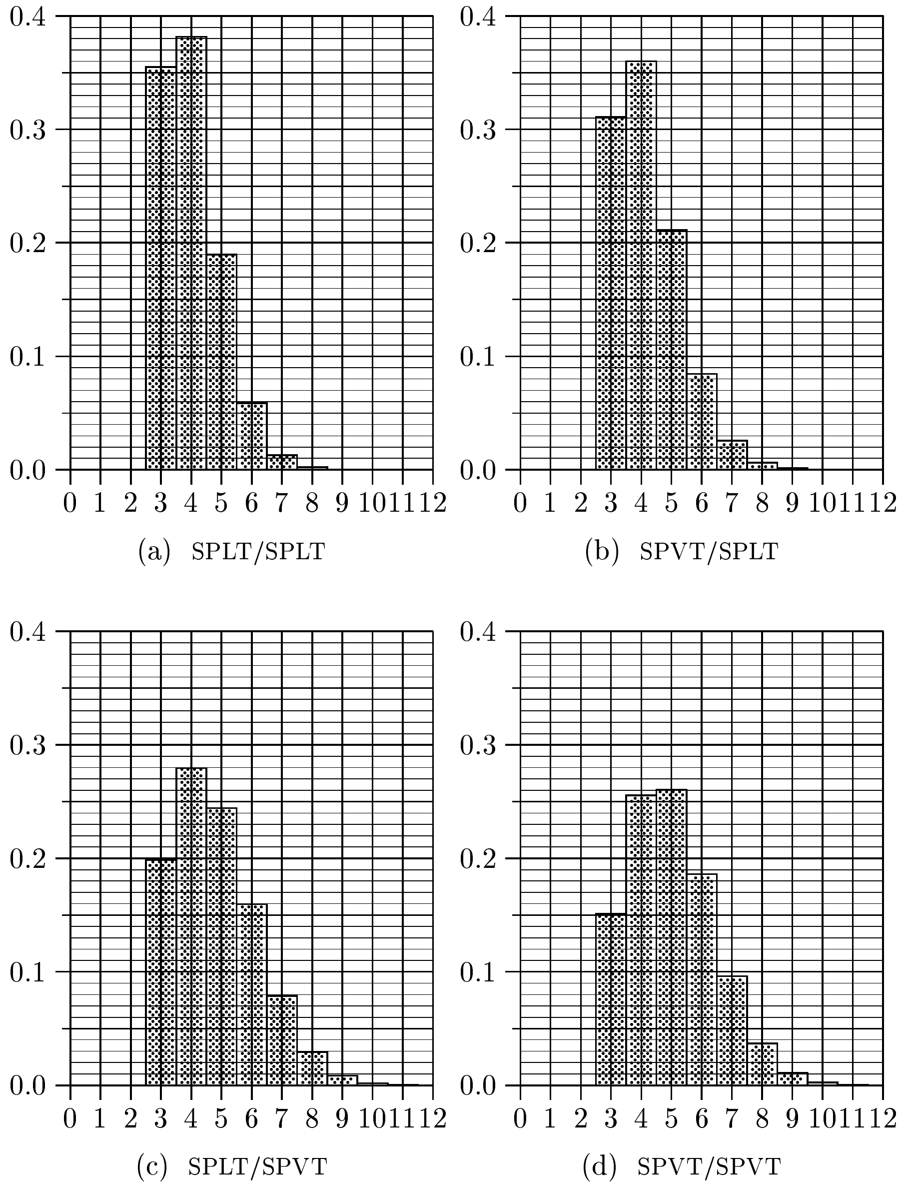

Figure 5: Histograms of relative frequencies of the number of vertices of the typical cell of X_0/X_1-nesting with $L_{A,0} = 1$ and $L_{A,1} = 2$

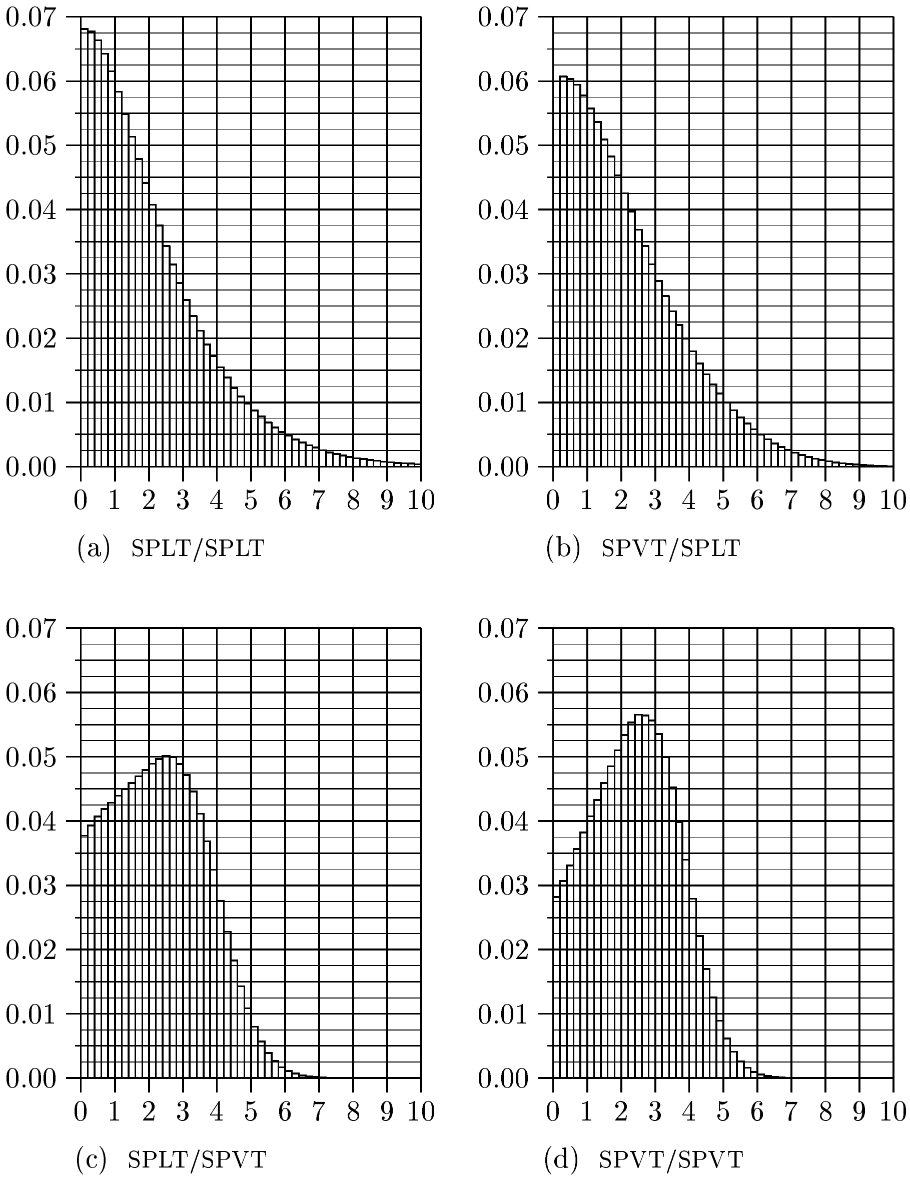

Figure 6: Histograms of relative frequencies of the perimeter of the typical cell of X_0/X_1-nesting with $L_{A,0} = 1$ and $L_{A,1} = 2$

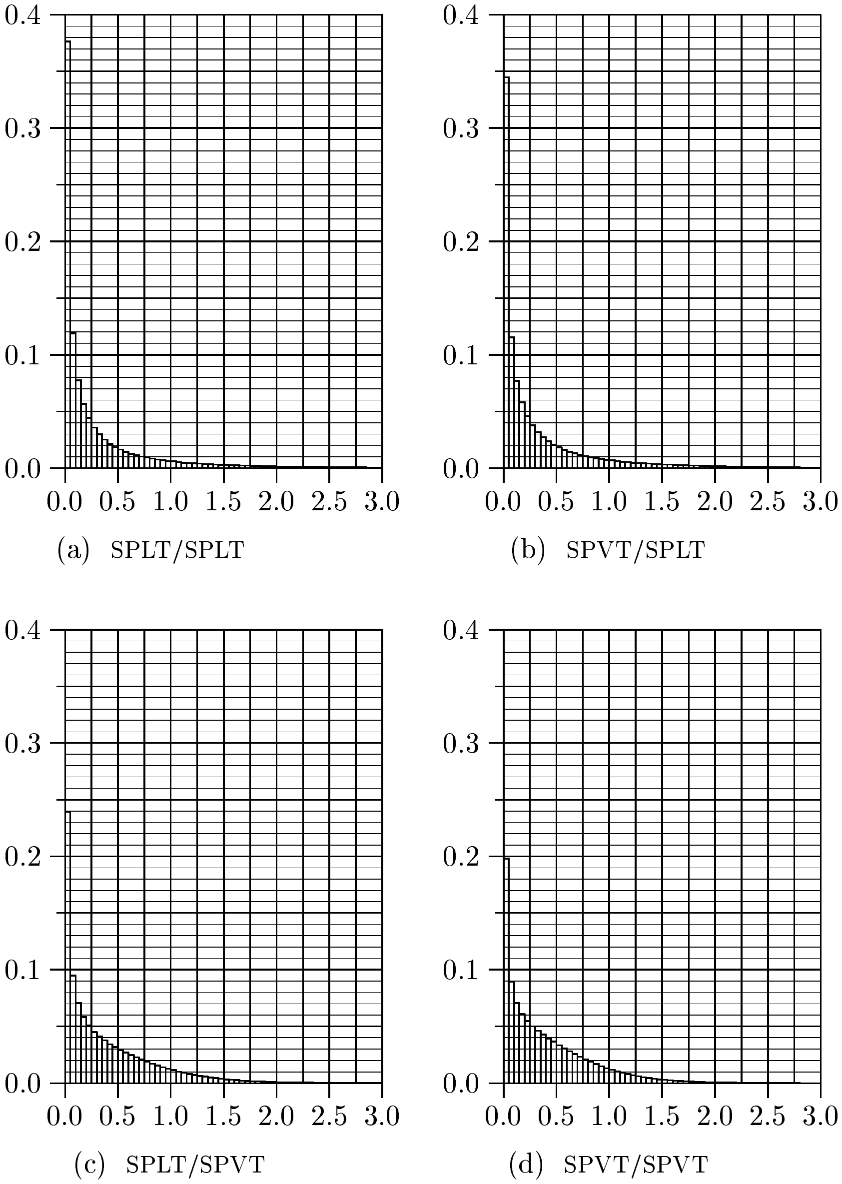

Figure 7: Histograms of relative frequencies of the area of the typical cell of X_0/X_1-nesting with $L_{A,0} = 1$ and $L_{A,1} = 2$

Using a SPVT as initial tessellation, the occurrence frequencies of triangles and quadrangles decrease. Cell shapes with five and more vertices occur more frequently; see Figure 5(b). This tendency is manifested in the obtained values for SPLT/SPVT-nesting. Here, the differences between the relative frequencies of SPVT/SPLT-nesting and SPLT/SPVT-nesting are caused by the reciprocal ratio of the expected total lengths of edges per unit area of the SPVT and SPLT. The histogram of relative frequencies of N in the case of SPVT/SPVT-nesting is most balanced of all, where quadrangles and pentagons have highest probability of occurrence; see Figure 5(b).

Consequently, a change in ratio $L_{A,1}/L_{A,0}$ in a SPLT/SPVT-nesting highly affects the shape of the typical cell. If we increase the ratio $L_{A,1}/L_{A,0}$, the shape of the typical cell is mainly influenced by the component tessellation SPVT and cells with more than five vertices appear more frequently. A decrease of the ratio $L_{A,1}/L_{A,0}$ affects a higher influence of the initial tessellation SPLT, and thus, an increasing relative frequency of cell shapes as triangles. The extreme cases are given in the cases of SPLT/SPLT-nesting and SPVT/SPVT-nesting.

There are great differences between the relative frequencies of U for different types of X_0/X_1-nesting; see Figure 6. A SPLT/SPLT-nesting produces more cells with very small and big perimeter. The relative frequencies of U of SPLT/SPLT-nesting are decreasing, whereas in a SPVT/SPVT-nesting the histogram is unimodal. As before, a change in the ratio $L_{A,1}/L_{A,0}$ in a SPLT/SPVT-nesting highly affects the perimeter of the typical cell within the two extreme cases of SPLT/SPLT-nesting and SPVT/SPVT-nesting. A decrease of the ratio $L_{A,1}/L_{A,0}$ affects an increasing relative frequency of cells with very small and big perimeter. A decrease of the ratio $L_{A,1}/L_{A,0}$ causes an increasing relative frequency of cells with higher perimeter with a unique maximum.

The shapes of the histograms of the relative frequencies of the cell area A are rather similar for the different types of X_0/X_1-nesting with $L_{A,0} = 1$ and $L_{A,1} = 2$ as shown in Figure 7. SPLT/SPLT-nesting and SPVT/SPVT-nesting have the highest and lowest relative frequency of small cells, respectively.

Roughly speaking, the relative frequencies of the geometrical characteristics N, U and A considered for the different types of X_0/X_1-nesting show the same qualitative behaviour. SPLT/SPLT-nesting and SPVT/SPVT-nesting produce the highest and lowest relative frequency of cells with a few number of vertices and of small perimeter and area, respectively. The shapes of the estimated densities for SPLT/SPVT-nesting and SPVT/SPVT-nesting strongly depends on the ratio $L_{A,1}/L_{A,0}$ of the expected total length of edges of the constituent tessellations per unit area. In contrast to the cell area A, the shapes of the estimated densities of N and U highly differ in the considered X_0/X_1-nestings. The development of statistical model tests which are based on the knowledge of N and U rather than on A seems appropriate for deciding the question, whether an SIT generated by SPVT and SPLT is suitable or not for observed empirical data.

Acknowledgement

This work was supported by France Telecom R&D through research grant no. 001B130.

References

[1] R.V. Ambartzumian (1990) *Factorization Calculus and Geometric Probability.* Cambridge University Press, Cambridge.

[2] F. Baccelli and P. Brémaud (1994) *Elements of Queueing Theory.* Springer-Verlag, Berlin, Heidelberg.

[3] F. Baccelli, C. Gloaguen and S. Zuyev (2000) Superposition of Planar Voronoi Tessellations. *Communications in Statistics, Ser. Stochastic Models* **16**, 69–98.

[4] D.J. Daley and D. Vere-Jones (1988) *An Introduction to the Theory of Point Processes.* Springer-Verlag, New York, 1988.

[5] E.I. George (1987) Sampling random polygons. *Journal of Applied Probability* **24**, 557–573.

[6] C. Gloaguen, P. Coupé, R. Maier and V. Schmidt (2002) Stochastic Modelling of Urbain Access Networks. *Networks 2002: 10th International Telecommunication Network Strategy and Planning Symposium*, München.

[7] O. Kallenberg (1983) *Random Measures.* Third Edition, Akademie Verlag, Berlin and Academic Press, London.

[8] W.S. Kendall and J. Mecke (1987) The range of the mean-value quantities of planar tessellations. *Journal of Applied Probability* **24**, 411–421.

[9] R. Maier and V. Schmidt (2003) Stationary iterated tessellations. *Advances of Applied Probability* **35**, 337-353.

[10] J. Mayer, V. Schmidt, and F. Schweiggert (2004) A Unified Simulation Framework for Spatial Stochastic Models. *Simulation Practice and Theory* (to appear).

[11] G. Matheron (1975) *Random Sets and Integral Geometry.* J. Wiley & Sons, New York.

[12] J. Mecke (1980) Palm methods for stationary random mosaics. In R.V.Ambartzumian (Eds.) *Combinatorial Principles in Stochastic Geometry.* Armenian Academy of Sciences Publishing House, Erivan, 124–132.

[13] J. Mecke (1981) Formulas for stationary planar fibre processes III – Intersections with fibre systems. *Math. Operationsf. Statist., Ser. Statistics* **12**, 201-210.

[14] J. Mecke (1984) Parametric representation of mean values for stationary random mosaics. *Math. Operationsf. Statist., Ser. Statistics* **15**, 437-442.

[15] R.E. Miles (1964) Random polygons determined by random lines in a plane. *Proc. Nat. Acad. Sci. USA* **52**, 901–907; 1157–1160.

[16] R.E. Miles (1972) The random division of space. *Advances in Applied Probability* , 243–266.

[17] R.E. Miles (1973) The various aggregates of random polygons determined by random lines in a plane. *Advances in Mathematics* **10**, 256–290.

[18] R.E. Miles (1974) A synopsis of Poisson flats in Euclidean spaces. In E.F. Harding and D.G. Kendall (Eds.) *Stochastic Geometry.* J.Wiley & Sons, New York, 202–227.

[19] R.E. Miles and M.S. Mackisack (2002) A large class of random tessellations with the class Poisson polygon distributions. *Preprint*, University of Sydney.

[20] J. Møller (1989) Random tessellations in $\mathbb{R}^d$. *Advances in Applied Probability* **21**, 37–73.

[21] A. Okabe, B. Boots, K. Sugihara and S.N. Chiu (2000) *Spatial tessellations. Concepts and Applications of Voronoi Diagrams.* Second edition. J. Wiley & Sons, Chichester.

[22] M.P. Quine and D.F. Watson (1984) Radial Generation of n-dimensional Poisson Processes. *Journal of Applied Probability*, **21**, 548–557.

[23] L.A. Santaló (1984) Mixed random mosaics. *Mathematische Nachrichten* **117**, 129–133.

[24] R. Schneider and W. Weil (2000) *Stochastische Geometrie.* Teubner, Stuttgart.

[25] V. Schmidt and R.F. Serfozo (1995) Campbell's formula and applications to queueing. In: J.H. Dshalalow (ed.) *Advances in Queueing: Theory, Methods and Open Problems.* CRC Press, Boca Raton, 225-242.

[26] D. Stoyan, W.S. Kendall, and J. Mecke (1995) *Stochastic Geometry and its Applications.* J.Wiley & Sons, Chichester.

[27] V. Weiss and W. Nagel (1999) Interdependences of directional quantities of planar tessellations. *Advances in Applied Probability* **32**, 664–678.